



OPEN

In situ gold adsorption experiment at an acidic hot spring using a blue-green algal sheet

Tatsuo Nozaki^{1,2,3,4✉}, Yasuyuki Fukushima⁵, Satoshi Okada⁶, Yutaro Takaya^{1,7,8}, Akiko Makabe⁶ & Masayuki Watanabe¹

Gold (Au), as one of the most precious metal resources that is used for both industrial products and private ornaments, is a global investment target, and mining companies are making huge investments to discover new Au deposits. Here, we report in situ Au adsorption in an acidic hot spring by a unique adsorption sheet made from blue-green algae with a high preferential adsorption ability for Au. The results of in situ Au adsorption experiments conducted for various reaction times ranging from 0.2 h to 7 months showed that a maximum Au concentration of 30 ppm was adsorbed onto the blue-green algal sheet after a reaction time of 7 months. The Au concentration in the hot spring water was below the detection limit (<1 ppt); therefore, Au was enriched by preferential adsorption onto the blue-green algal sheet by a factor of more than $\sim 3 \times 10^7$. Thus, our gold recovery method has a high potential to recover Au even from an Au-poor solution such as hot spring water or mine wastewater with a low impact on the environment.

The contemporary world gold reserves are estimated to be about 52000 tons¹, which corresponds a volume of less than that of one Olympic-sized swimming pool. At present, gold is produced mainly from epithermal Au–Ag, placer, and orogenic gold deposits, as a byproduct from porphyry copper (Cu), volcanogenic massive sulfide, or other hydrothermal deposits^{2–6}, and by recycling from the urban mine. The total annual Au production from these sources was 3090 tons in 2021 and 3100 tons in 2022¹; thus, assuming the same reserve and annual production rate in the future, the reserve to production ratio can be estimated to be only about 17 years. For this reason, mining and metal companies are investing large amounts of money to discover new Au deposits to ensure a stable and diversified supply of Au resources. As the number of newly discovered large metal deposits has decreased, biosorption techniques for metal elements such as Cd, Cu, Ni, Pb, and Zn have become attractive for recovering metal elements with a low impact on the environment^{7–11}. In particular, some blue-green algae with a high preferential adsorption ability for Au have been utilised in biosynthesis experiments to produce gold nanoparticles^{12–15}.

Filamentous blue-green algae living in alkaline and Na–Si–Ca–S–K–B-rich hot spring waters in northeastern Japan with temperatures ranging from 50 to 60 °C and a pH of 8–9 are known to have a high preferential adsorption ability for Au^{16–18}. These blue-green algae, which have been classified into the genus *Leptolyngbya* by 16S ribosomal DNA analyses and BLASTn (Nucleotide Basic Local Alignment Search Tool) searches, are possibly *L. laminosa*¹⁸. The maximum amount of Au adsorption has been estimated to be 0.31 kg per kg algae, and Au was well adsorbed even onto dead, desiccated algae^{16–18}. We thus hypothesised that a sheet of dry, dead algae could be used as a concentrator for Au, even from an Au-poor solution. We therefore conducted in situ experiments in

¹Research Institute for Marine Resources Utilization, Submarine Resources Research Center, Japan Agency for Marine–Earth Science and Technology (JAMSTEC), 2-15 Natsushima-cho, Yokosuka 237-0061, Japan. ²School of Engineering, Frontier Research Center for Energy and Resources, The University of Tokyo, 7-3-1 Hongo, Bunkyo-ku, Tokyo 113-8656, Japan. ³Department of Planetology, Graduate School of Science, Kobe University, 1-1 Rokkodai-cho, Nada-ku, Kobe 657-8501, Japan. ⁴Department of Earth and Environmental Sciences, Faculty of Science, University of Ottawa, 25 Templeton Street, Ottawa, ON K1N 6N5, Canada. ⁵Applied Physics and Chemistry Group, Technology Platform Center, Technology and Intelligence Integration, IHI Corporation, 1 Shin-nakahara-cho, Yokohama 235-8501, Japan. ⁶Super-cutting-edge Grand and Advanced Research Program, Japan Agency for Marine–Earth Science and Technology (JAMSTEC), Institute for Extra-cutting-edge Science and Technology Avant-garde Research (X-Star), 2-15 Natsushima-cho, Yokosuka 237-0061, Japan. ⁷Department of Systems Innovation, School of Engineering, The University of Tokyo, 7-3-1 Hongo, Bunkyo-ku, Tokyo 113-8656, Japan. ⁸Faculty of Science and Engineering, Waseda University, 3-4-1 Okubo, Shinjuku-ku, Tokyo 169-8555, Japan. ✉email: nozaki@jamstec.go.jp

which we used algal sheets for Au adsorption (recovery) from acidic hot spring water (Fig. 1a), such a trial result about the Au recovery from acidic hot spring water has been quite limited so far. At the end of the longest in situ adsorption experiment of 7 months, the Au concentration on the blue-green algal sheet was up to about 30 ppm; this concentration is much higher than that of the typical cut-off grade (6–8 ppm¹⁹) for Au deposits on land.



Figure 1. In situ Au adsorption experiment. (a) Blue-green algal sheets were attached to the bottom and sides of a PFA basket (30 cm by 25 cm by 15 cm high). Then, the PFA basket was set on an overturned plastic basket to prevent the blue-green algal sheets from being buried under hot spring water precipitate (sinter deposits). To prevent corrosion and contamination, no metal pieces were used. (b–d) Photographs taken (b) just before and (c, d) after the blue-green algal sheets and PFA basket were put into the test water tank at the Neutralisation Treatment Facility at Tamagawa Hot Spring. Hot spring water with a temperature of 60 °C and a pH of 1.2 flowed through the tank at a rate of 6 m³/h. (e) The blue-green algal sheets after the 7-month in situ Au adsorption experiment in the test water tank. The yellowish precipitate is a sinter deposit dominated by native sulfur. (f) The blue-green algal sheets just after they were washed with tap water to remove the sinter deposit.

Tamagawa hot spring

The in situ Au adsorption experiments were performed in a test water tank located in the Tamagawa Neutralisation Treatment Facility, Tamagawa Hot Spring, Akita Prefecture, northeastern Japan (Fig. 1b–d). Tamagawa Hot Spring has been active for more than 300 years. It is one of the most acidic hot springs in Japan, with a temperature of 98 °C, a pH of 1.2, a discharge rate of 9000 L/min, and a heat discharge of 1.8×10^{15} J/year^{20–24}. The hot spring is associated with an old sulfur mine²⁵ and with occurrences of the rare mineral hokutolite [(Ba,Pb)SO₄]²⁶. It is rich in both Cl and SO₄, but Cl is usually dominant (for example, at Obuki, the largest discharge site, Cl = 4020 ppm and SO₄ = 1730 ppm in 2007²³). From its oxygen ($\delta^{18}\text{O}$) and hydrogen (δD) isotopic compositions, the hot spring water at Obuki has been inferred to experience boiling (phase separation) at several tens to several hundreds of meters below ground^{20,23}. It also contains volcanic gas derived from deeper magma with an estimated mixing ratio of volcanic gas to meteoric water of 1:5^{20,23}. We chose Tamagawa Hot Spring as the site for our in situ Au adsorption experiment because the solubility of gold is known to increase exponentially with increasing temperature and decreasing pH^{27,28}.

The acidic hot spring water is neutralised by lime (pH > 3) at the Neutralisation Treatment Facility to protect the flora and fauna in Tamagawa Dam Lake and downstream²⁴. Because it was not possible to conduct in situ Au adsorption experiments at the Obuki hot spring source, we used a test water tank at the Neutralisation Treatment Facility, which is about 600 m downstream from the hot spring source (Fig. 1b–d). The temperature and pH of the hot spring water flowing into the test water tank are 60 °C and 1.2, respectively²⁹.

Materials and methods

To make algal adsorption sheets for Au, incubated blue-green algae were washed with tap water, a hydrochloric acid solution, and then tap water again, followed by oven-drying^{17,18}. The blue-green algae for the adsorption sheets were packed into a fiberglass mesh, and the adsorption sheets were then attached to the bottom and sides of an acid-resistant, perfluoroalkoxy (PFA) basket by nylon strings without any metal parts, which are easily corroded and destroyed by the acidic hot spring water. The PFA basket was placed on an overturned plastic basket to prevent burial of the Au adsorption sheets by hot spring water precipitates (sinter deposits). The basket with the Au adsorption sheets was immersed in a test water tank through which hot spring water flowed at a rate of 6 m³/h and the water above the certain level flowed out from the tank via the standpipe (Fig. 1d) for various treatment periods (0, 0.2, 0.5, 1, 3, 6, and 13 h; 1, 2, 3, 4, 5, 6, and 7 days; 2 and 3 weeks; and 1, 2, 3, and 7 months) so that secular changes in the adsorbed element concentrations could be observed. After each in situ experiment, the sheets were immediately washed with tap water to remove the yellowish, sulfur-rich precipitate from the surface (Fig. 1e, f).

The algal adsorption sheets were then brought back to the laboratory, where they were washed well again with tap water, dried, and then split into two parts, together with the removal of the fiberglass mesh. One part was used for microscopic observations, and the other was pulverised for geochemical analysis. The surface structure, texture, and precipitated minerals on the adsorption sheets were observed by field emission-scanning electron microscopy (FE-SEM) and energy-dispersive X-ray spectroscopy (EDS)³⁰. The element concentrations on the adsorption sheets and in the precipitate were determined by inductively coupled plasma-mass spectrometry (ICP-MS) with the mixed acid digestion method^{31,32} (Supplementary Table S1). The chemical composition of the hot spring water source at Obuki was determined by ion chromatography (IC) and ICP-atomic emission spectrometry (ICP-AES)³³ (Supplementary Table S2), and the chemical composition of the hot spring water in the test water tank was determined by ICP-MS at Japan Agency for Marine-Earth Science and Technology (JAMSTEC)³⁴ (Supplementary Table S3) and by ICP-MS and high-resolution (HR)-ICP-MS at Activation Laboratories Ltd., a commercial analytical service (Supplementary Table S4).

Results and discussion

SEM observations of the adsorption sheets

During the in situ Au adsorption experiment, the blue-green algal adsorption sheets became smaller and thinner than the starting material, and their dry weights decreased exponentially with the reaction time (Fig. 2). At 24 h, the weight of the adsorption sheets had decreased to 73% of that of the starting material (a 27% weight loss), and at 168 h (1 week), 68% of the weight had been lost (Fig. 2). At 2 weeks, the weight loss had slowed and almost plateaued, and at 2–3 months, only 18–19% of the original weight remained. No weight change data are available from the 7-month experiment (Fig. 2). In addition to the weight loss, the surface structure and texture of the adsorption sheets changed with time (Supplementary Figs. S1 and S2). Initially, clear filamentous and tube-like structures ~ 1 µm in diameter derived from the blue-green algae could be observed by FE-SEM, but after one week, these structures became vague and unclear (Supplementary Figs. S1 and S2a, b). After 7 months, the filamentous structures became fragmented, and the fragments then aggregated and were partly covered by the precipitated minerals; the end result was a massive sheet-like structure (Supplementary Figs. S1 and S2c, d).

The major constituent minerals observed on the blue-green algal sheet were determined by SEM-EDS to be barite (BaSO₄), halite (NaCl), and a silica mineral, along with minor unidentified Ca and Fe silicates, Fe-oxide (or oxyhydroxide?), As-S minerals, and galena (PbS) (Fig. 3a, b and Supplementary Fig. S3). Among these minerals, barite was the most abundant and exhibited a euhedral shape and high crystallinity (Fig. 3a, b). The silica mineral species could not be determined only by SEM-EDS observation, but in hot spring water with a pH of 1.2 and a temperature of 60 °C, opal plausibly precipitates, as at Shinyu, Tateyama Hot Spring, Toyama Prefecture, Japan³⁵. The Au-rich grains were not euhedral but rounded (Figs. 3c and 4a) or irregular in shape, with a maximum size of ~ 1 µm (Figs. 3d–f and 4b, c). In a laboratory experiment using blue-green algae and a HAuCl₄ solution, nano-scale Au grains with a typical size of several tens of nanometers were initially precipitated^{17,18}; therefore, the presence of large Au grains of several hundred nanometers on the blue-green algal sheet indicates

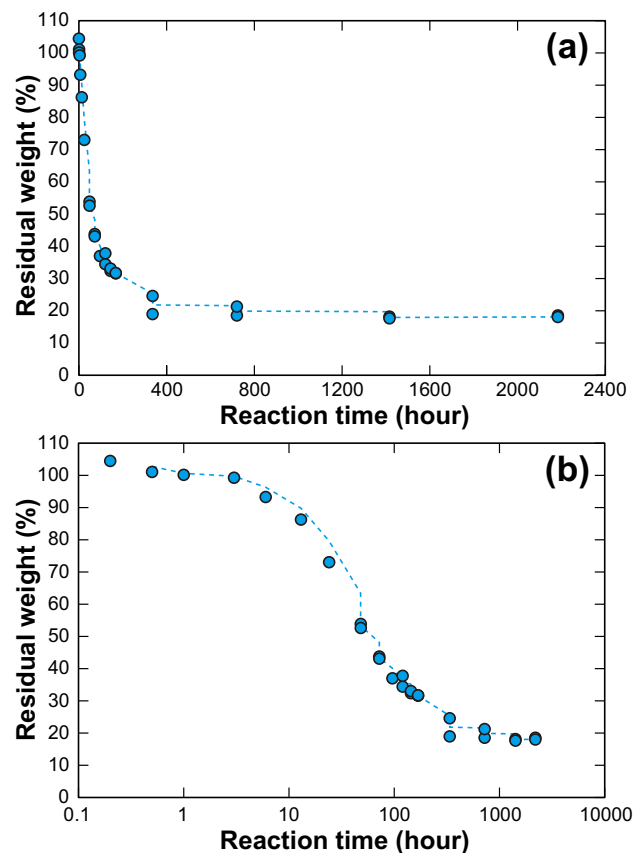


Figure 2. Residual weight (relative to the starting weight) of the blue-green algal sheets in relation to reaction time. In (a), the horizontal axis scale is linear, and in (b), it is logarithmic. The blue dashed lines represent the two-point moving average.

overgrowth of Au nano-particles (Figs. 3c–f and 4a–c). One Au-rich grain had an angular rounded shape under the FE-SEM observation (Figs. 3c and 4a). Native gold has an isotropic structure (Fm3m³⁶), but this Au-rich grain does not have an isotropic morphology. The largest Au grain in our FE-SEM observations (Figs. 3d and 4b) had a rod-like, filamentous shape reflecting the continuous overgrowth of the Au grain along the original filamentous shape of the blue-green algae during the 7-month in situ adsorption experiment.

Elemental mapping by SEM–EDS (Fig. 4 and Supplementary Fig. S3) showed that the Au-rich grains did not contain any Ag, but they often included some Ni or As and S, as well as C, N, O, Al, and Si, which were partly derived from the blue-green algae themselves or due to background noise from reflected electrons. Some of the Au grains were overgrowth on barite or silica mineral grains (Figs. 3e, f and 4c). Au nano-particles with a width of 15–30 nm attached to the surface of one massive, irregularly shaped Au-rich grain (Fig. 3f) resulted from (1) the simultaneous formation of Au nano-particles (nuclei of larger Au grains) at the adsorption sheet surface or (2) overgrowth of existing Au nano-particles/grains during continuous mineralisation in hot spring water.

Au adsorption on the blue-green algal sheets

The Cl and SO₄ concentrations in the hot spring water source at Obuki were 94.91 mM (3365 ppm) and 14.04 mM (1348 ppm), respectively (Supplementary Table S2); thus, the SO₄ [ppm] / Cl [ppm] ratio was ~0.4. The Tamagawa hot spring water is a Cl–SO₄-mixed type, but, consistent with previous studies^{21,23}, it is dominated by Cl rather than by SO₄. The Au concentrations of the hot spring water in the test water tank determined by ICP–MS were all below the detection limit, and those determined by HR–ICP–MS at Activation Laboratories Ltd. were also below the detection limit (< 1 ppt), except for one sample (THS–UF3; Supplementary Tables S3 and S4). The concentrations of elements in the hot spring water did not differ greatly between the filtered and unfiltered samples.

Bulk geochemical compositions of the blue-green algal sheets after the in situ Au adsorption experiment are shown in Fig. 5 and Supplementary Table S1. Elements with maximum concentrations exceeding 0.1 wt% (1000 ppm) after 7 months were Al (0.17 wt%), Ti (0.16 wt%), Fe (0.13 wt%), As (0.39 wt%), Ba (0.78 wt%), and Pb (0.19 wt%). The Ba concentrations in the hot spring water in the test water tank were only 0.3–0.5 ppm, much lower than those of the other major elements such as Na, Mg, Al, K, Ca, and Fe (> 20 ppm) (Supplementary Tables S3 and S4). However, on the adsorption sheets, barite was the most abundant mineral, and the Ba concentration was the highest, because barite could easily form from the abundant SO₄²⁻ ions in the hot spring water and, once formed, was a stable/intact mineral. Secular changes in the bulk geochemical compositions of the adsorption sheets exhibited four behaviors: (1) an exponential increase (e.g., As, Au, and Pb); (2) a linear

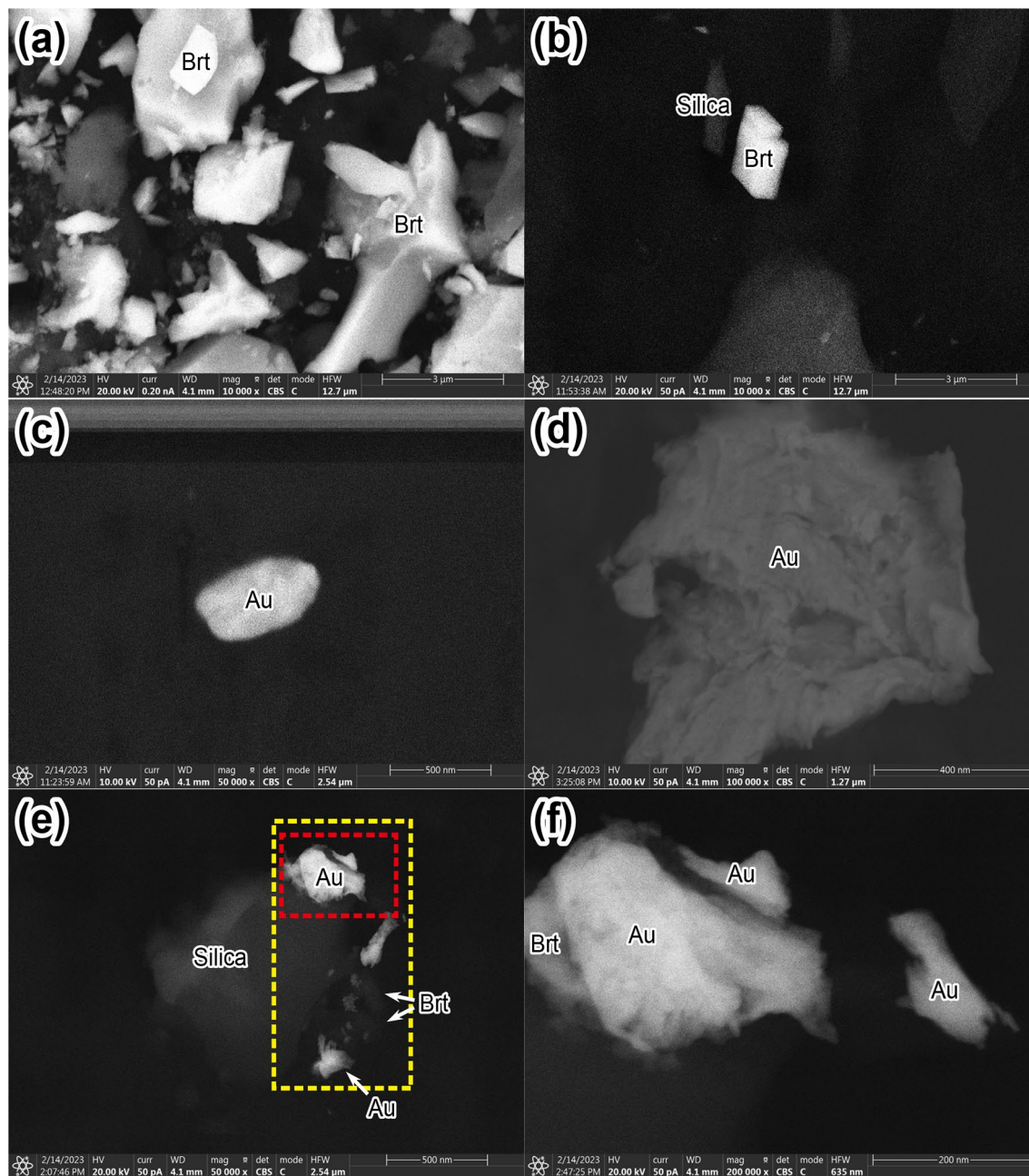


Figure 3. SEM images of a blue-green algal sheet after the 7-month in situ Au adsorption experiment. (a) Abundant barite grains. (b) A euhedral barite grain with a silica mineral grain. (c–f) Au-rich grains formed on the blue-green algal sheet. (f) An enlarged image of the grain within the red dotted rectangle in (e). The yellow dotted square indicates the area of the SEM–EDS elemental mapping shown in Fig. 4c. Brt, barite; Au, Au-rich grain.

increase (e.g., Fe, In, and Sn); (3) a linear decrease (only P); and (4) an exponential increase till ~ 12 h followed by a gradual decrease (e.g., Sc and Th) (Fig. 5 and Supplementary Table S1). These different behaviors indicated that some elements were continuously adsorbed onto the blue-green algal sheets during the in situ adsorption experiment, whereas the concentrations of other elements reached an adsorption limit. The linear decrease in the P concentration is attributable to the destruction and dissolution of the original P-bearing filamentous structure of the blue-green algae (Supplementary Figs. S1 and S2). The Au concentrations on the blue-green algal sheets were the highest after the 7-month experiment (10.35, 12.18, 15.70, and 30.01 ppm; Fig. 5 and Supplementary Table S1). The adsorption sheet attached to the bottom of the PFA basket had an Au concentration of 15.70 ppm, and the maximum value of 30.01 ppm was recorded on one of the adsorption sheets attached to the side of the PFA basket (Supplementary Table S4). Although in the laboratory experiment using the 0.5–100 ppm HAuCl_4 solution with a pH of ~ 0.7 to 4 adjusted by the HCl solution or aqua regia at room temperature (~ 25 °C), the limit of Au adsorption was reached in only ~ 10 h because of the formation of many Au nano-particles^{16–18}, in the

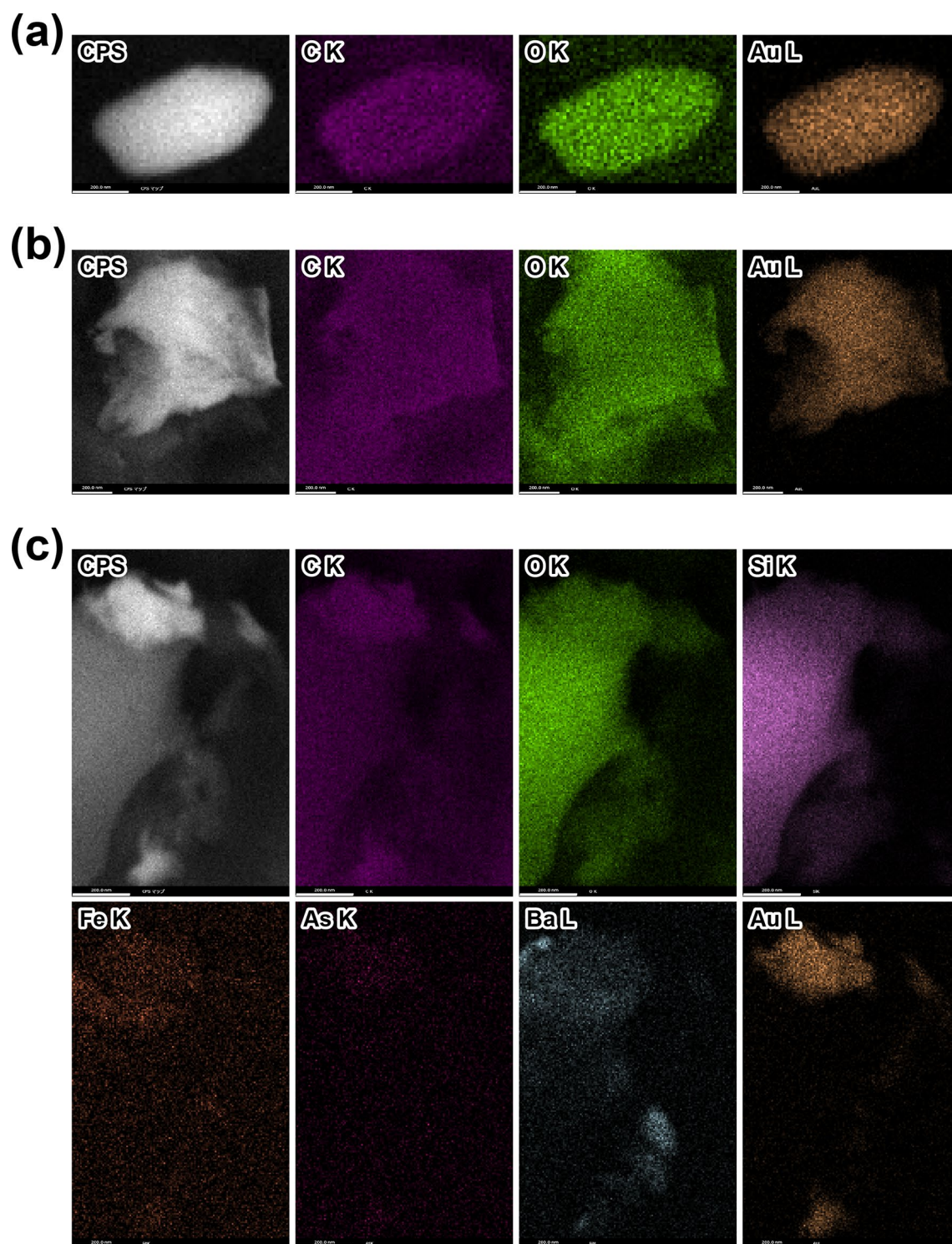


Figure 4. SEM-EDS elemental mappings. (a–c) Mapping results for the Au-rich grains shown in Fig. 3c–e. The EDS elemental maps were obtained from the L lines for Ba and Au and from the K lines for other elements. X-ray counts per second (CPS) maps were also obtained. White scale bars indicate 200 nm.

in situ adsorption experiments in the test water tank, the Au concentration was still increasing after 7 months (Fig. 5 and Supplementary Table S1). In the laboratory experiment using the HAuCl_4 solution, the high initial concentration of dissolved Au induced fast nucleation followed by the growth of Au particles until the dissolved Au was used up^{16–18,37}. In contrast, in the hot spring water in the test water tank, the dissolved Au concentration was extremely low (below the detection limit); therefore, the precipitation of Au was controlled by the limited initial nucleation, and overgrowth then occurred preferentially on the previously formed nuclei (Figs. 3c–f and 4). The Au concentration is highly correlated (correlation coefficient $r > 0.7$) with elemental concentrations of Sr

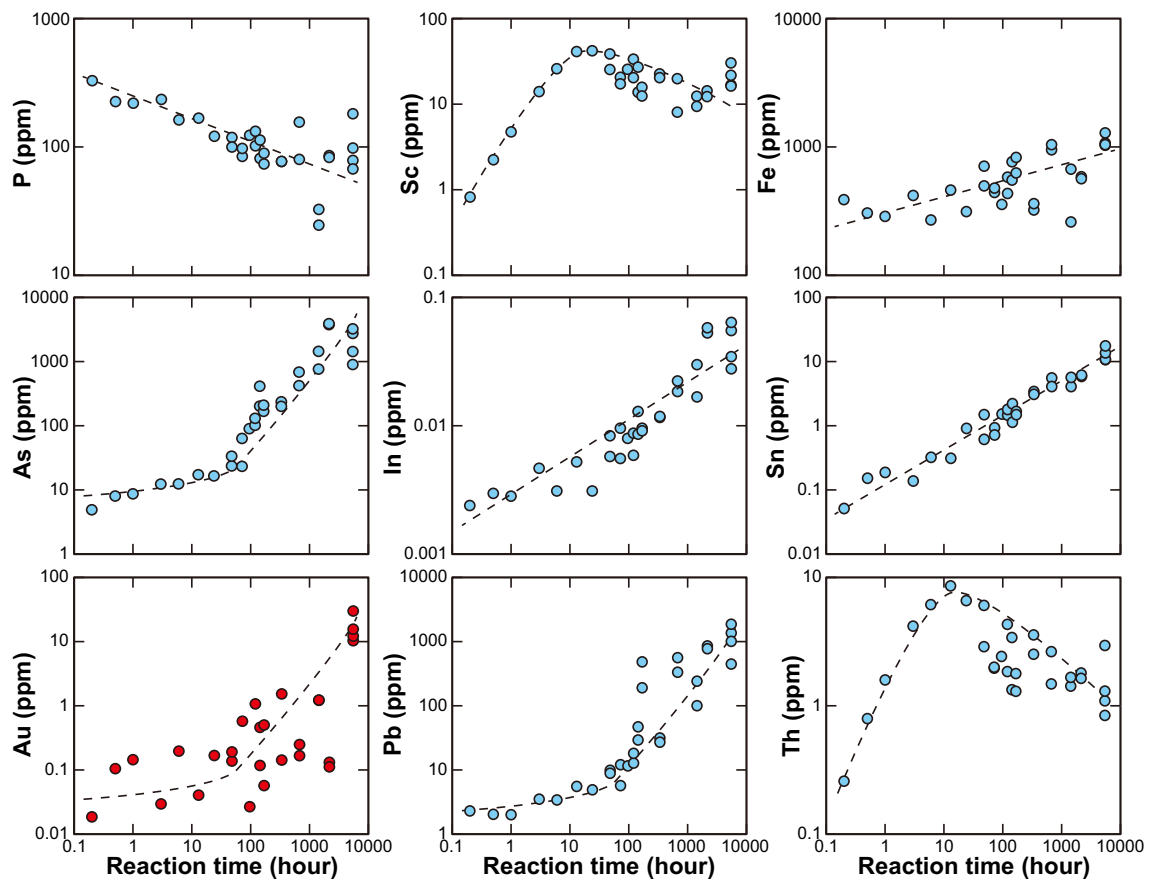


Figure 5. Secular changes in element concentrations. The changes with time of the concentrations of each element adsorbed onto the blue-green algal sheet show four patterns: (1) an exponential increase (As, Au, and Pb), (2) a linear increase (Fe, In, and Sn), (3) a linear decrease (P), and (4) an exponential increase followed by a gradual decrease (Sc and Th).

($r=0.75$), Cd (0.71), Sn (0.76), Ba (0.74), Pb (0.76), and Bi (0.72), followed by Ag (0.68). These elements are well known to be enriched in sulfide and sulfate minerals, and such enrichment is consistent with our microscopic observations of abundant barite with minor galena (Fig. 3a, b).

The following elements had concentrations higher than 0.1 wt% in the hot spring water precipitate (sinter deposit) in the test water tank: Al (0.20 wt%), Ti (0.18 wt%), Fe (0.16 wt%), As (1.21 wt%), and Pb (0.55 wt%). In addition, the concentrations of Sb (295 ppm) and Ba (688 ppm) were relatively high (Supplementary Table S1). On the blue-green algal sheets, the concentrations of Ba and As were the highest and second highest, respectively, whereas in the hot spring water precipitate, those of As and Pb were the highest and second highest, respectively, and the Ba concentration (688 ppm) was one order of magnitude lower than the maximum Ba concentration (0.78 wt%) on the blue-green algal adsorption sheet. Thus, the blue-green algae induced selective and preferential adsorption and precipitation of minerals from the hot spring water. In particular, the Au concentration in the hot spring water precipitate was only 0.017 ppm, which is $\sim 1/1700$ of the maximum Au concentration on the blue-green algal sheets (~ 30 ppm) after 7 months. This result indicates that most of the Au in the hot spring water in the test water tank that was not adsorbed onto the blue-green algal sheet did not precipitate as Au-rich grains but was released downstream.

To understand the preferential adsorption onto the blue-green algal sheet, bulk geochemistry enrichment factors were calculated by normalizing concentrations to those in (1) the hot spring water or (2) the hot spring water precipitate (sinter deposit) in the test water tank (Figs. 6a, b). If element concentrations in the hot spring water were below the detection limit ($<^{**}$ $\mu\text{g/L}$ or ng/L ; Supplementary Table S4), we used the detection limits to calculate the average compositions of the hot spring water for the purposes of normalisation (note that the Au value of sample THS-UF3 was an outlier and was removed from the calculations). Thus, the enrichment factors of those elements represent minimum values (Fig. 6a). The P and Zn concentrations in the hot spring water precipitate determined by ICP-MS were also below the detection limit; therefore, these data were also removed from the enrichment factor calculations (Fig. 6b). The enrichment factors calculated by normalisation to the hot spring water exceeded 10^5 for five elements: Au was enriched the most relative to the hot spring water, by 3.0×10^7 ; Ti was enriched by 1.0×10^5 , Cu by 1.3×10^6 , Zr by 1.3×10^5 , and Nb by 1.6×10^6 (Fig. 6a). Other enriched elements included Ni (by 3.0×10^4), Ag, (1.5×10^4), Sn (3.5×10^4), Te (4.6×10^4), Ba (2.6×10^4), Hf (3.9×10^4), and Bi (1.1×10^4). Among these elements, Zr, Nb, and Hf are compatible with refractory minerals such as zircon, whereas Cu, Au, Ni, Ag, Sn, Te, Ba, and Bi tend to be enriched in sulfide and sulfate minerals. Although

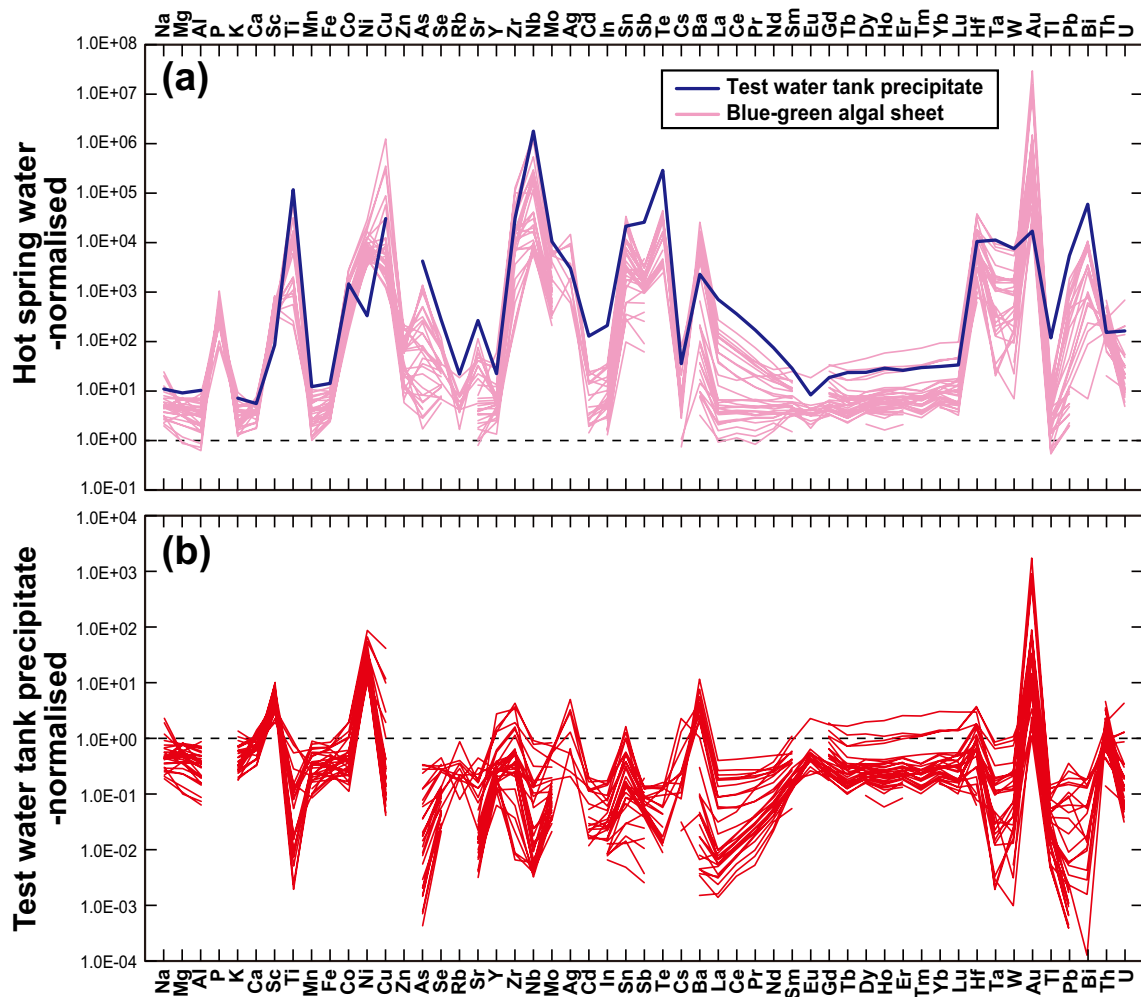


Figure 6. Bulk geochemistry enrichment results. Enrichment was calculated by normalizing the concentration on the blue-green algal sheets by the concentration in (a) hot spring water or that in (b) the sinter deposit in the test water tank. The average concentration of the six hot spring water samples (Supplementary Table S4) was used as the normalizing value. For Au only, the concentration in sample THS-UF3 was removed as an outlier when the average concentration was calculated. For concentrations of elements in the hot spring water below the detection limit, we used the detection limit to calculate the average concentrations. The enrichment factors of these elements may therefore be underestimates.

12 elements were enriched on the adsorption sheets more than 10^4 -fold relative to the hot spring water, only a few elements were more enriched on the adsorption sheets than in the hot spring water precipitate (Fig. 6a). Calculation of enrichment by normalisation to the hot spring water precipitate allowed clear visualisation of the elements that were released downstream or well adsorbed onto the blue-green algal sheet (Fig. 6b). Only four elements were enriched more than ten-fold relative to the precipitate: Ni (8.5×10^1), Cu (4.0×10^1), Ba (1.1×10^1), and Au (1.7×10^3). Among these four elements, Au was more enriched than the other elements by two orders of magnitude; this result demonstrates that the blue-green algal sheet showed strong preferential and selective adsorption ability for Au even from an Au-poor liquid such as hot spring water with an Au concentration below the detection limit. It should be noted that, when normalised to the hot spring water precipitate, As and Pb are not enriched onto the blue-green algal sheet, with their enrichment factors of less than 1 (Fig. 6b), indicating that these toxic elements were not preferentially and selectively adsorbed on the blue-green algal sheet.

The exponential weight loss of the adsorption sheets during the experiment (Fig. 2) indicates that their durability needs to be improved for a more stable Au recovery method. Moreover, the adsorption behavior of the blue-green algae in an Au-poor solution with various combinations of dominant elements (components) should be investigated through more laboratory experiments, as well as the effective method of Au extraction from the blue-green algal sheet such as acid leaching and/or burning¹⁸. Nevertheless, our results demonstrate that our Au recovery method using an adsorption sheet made from blue-green algae has high potential for the future recovery of Au even from Au-poor solutions such as hot spring water, sewage water, mine wastewater, and seafloor hydrothermal fluid with a low impact on the environment.

Conclusions

After a 7-month in situ adsorption experiment in acidic hot spring water, the Au concentration adsorbed onto the blue-green algal sheets was as high as ~30 ppm. The minimum enrichment of Au relative to its concentration in the hot spring water in the test water tank was estimated to be ~ 3×10^7 fold; this value is one or two orders of magnitude higher than the enrichment value of other elements in the hot spring water. Furthermore, relative to the hot spring water precipitate, Au was enriched the most, by 1.7×10^3 , followed by Ni, Cu, and Ba. Thus, the blue-green algal sheets maintained their high preferential and selective adsorption ability for Au even from an Au-poor solution (Au below the detection limit) and in the presence of other major elements (Na, Mg, Al, K, Ca, and Fe > 20 ppm). Therefore, the Au recovery method using blue-green algal adsorption sheets has a high potential to recover Au from Au-poor resources.

Methods

Sample preparation for Au adsorption experiment

Blue-green algae collected from an alkaline hot spring in northeastern Japan were incubated in the laboratory in alkaline water (pH = 9–10) with liquid fertiliser at room temperature (~25 °C)^{17,18}. After incubation, the incubated blue-green algae were washed with tap water for 10 min several times to remove any remaining liquid fertiliser. Then, the algae were washed with a 2-M HCl solution for 10 min to remove unwanted components and enhance the Au adsorption ability and with tap water for 10 min several times to wash out the HCl solution and dried at 60 °C in an oven. The 7-month in situ adsorption experiment was performed from 15 October 2021 to 1 June 2022 because the Tamagawa Hot Spring is inaccessible during the winter because of heavy snow. The 2-month and 3-month experiments were begun on 9 August 2022, and the other, shorter term experiments were begun on 30 September or 1 October 2022. It should be noted that incubation batches of blue-green algae used in the in situ adsorption experiments and the starting and ending times of the experiments were not necessarily the same.

Microscopic observations by FE-SEM

Scanning electron microscopy (SEM) imaging and energy-dispersive X-ray spectroscopy (EDS) analyses were performed in a Helios G4 UX system (Thermo Fisher Scientific Inc.) equipped with an EDS detector (Octane Elite Super (C5), Ametek) at JAMSTEC³⁰. A 3-mm-diameter disc of a blue-green algal sheet was punched out and pasted onto an aluminum stub using double-sided carbon tape. Secondary electron (SE) imaging of the morphology of the adsorption sheets was performed at 1 kV, and SE and backscattered electron (BSE) imaging and EDS analyses of the constituent minerals were performed at an acceleration voltage of 10 or 20 kV without any conductive coatings. EDS elemental maps were obtained from L lines for Ba and Au, and from K lines for other elements; X-ray counts per second (CPS) maps were also obtained (Fig. 4 and Supplementary Fig. S3). For the SEM image shown in Supplementary Fig. S2b, the recovered sample was further rinsed with Milli-Q deionised water, dried under vacuum, embedded in epoxy resin, sectioned to a thickness of 1 µm using an ultramicrotome (UC7, Leica), and collected onto a copper grid. SEM–EDS imaging was performed at an acceleration voltage of 20 kV. The cross-correlation between the EDS maps of two elements A and B ($I_{XC}(A, B)$) was calculated as follows:

$$I_{XC}(A, B)_{ij} = [I_A]_{ij} \cdot [I_B]_{ij} / \sum_{ij} ([I_A]_{ij} \cdot [I_B]_{ij})$$

where $[I_X]_{ij}$ denotes the intensity of element X at pixel (i, j)³⁸.

Major and trace element analyses by IC, ICP-AES, and (HR-)ICP-MS

Natural hot spring water at Obuki was collected on 14 October 2021 by the research group of Tohoku University. We brought back a hot spring water sample in a glass bottle to the laboratory without filtering or acid addition, because the pH of the hot spring water was low enough at 1.2. Hot spring water was collected from the test water tank on 30 September 2022 in two PFA bottles, one with filtering through an EMD Millipore membrane syringe filter (0.45 µm pore size, 25 mm diameter) and one without filtering (samples THS-F and THS-UF, respectively; Supplementary Tables S3 and S4). Each of the two hot spring water samples were then split into three subsamples for analysis (THS-F1–F3 and THS-UF1–UF3).

The mass fractions of the major constituents in the natural hot spring water collected at Obuki (Supplementary Table S2) were measured with an ion chromatography (IC) system (Dionex ICS-1600 or ICS-2100; Thermo Fisher Scientific Inc.) and an ICP-AES system (SPECTRO ARCOS; SPECTRO Analytical Instruments Inc.) at JAMSTEC after appropriate sample filtering and dilution with Milli-Q deionised water, following the method of Miyazaki et al.³³. These results were calibrated by using diluted reference solutions made with the ICP Multi-element Standard IV Certipur® (Merck), the Anion Mixture Standard Solution I, the Cation Mixture Standard Solution III, the Chloride Ion Standard Solution (Cl⁻ 1000) and the Sodium Standard Solution (Na 1000) (FUJIFILM Wako Chemicals).

Major and trace element analyses of the blue-green algal sheets and the hot spring water in the test water tank (Supplementary Tables S1 and S3) were performed by ICP-MS with an Agilent 7500ce system installed at JAMSTEC. Powdered samples weighing ~50 mg (1 mL of hot spring water) were dissolved by the HNO₃-HClO₄-HF digestion method in Teflon PFA screw-cap beakers and then heated overnight on a hot plate at 110 °C. The digested samples were progressively evaporated at 110 °C for more than 12 h, at 130 °C for 3 h, and at 160 °C until dryness. The residue was dissolved in 5 mL of Milli-Q deionised water combined with 4 mL HNO₃ and 1 mL HCl, and then further diluted to 1:100 or 1:20 by mass (total dilution factor ~20,000 or ~200) before introduction into the ICP-MS system. Details of these analytical procedures, including instrumental drift and mass interference correction methods, are reported in Takaya et al.³¹ and Nozaki et al.^{32,34}.

The hydrogeochemistry of the hot spring water in the test water tank (Supplementary Table S4) was also analysed by ICP-MS or HR-ICP-MS at Activation Laboratories Ltd., Canada, using the following packages: Code 6 (Total Recoverable Natural Waters with low TDS [total dissolved solids] [$<0.05\%$]), Code 6 Overage (Over-range elements in Code 6 MB [marine water, brines, or other aqueous solution with TDS $>0.05\%$ reanalysed by ICP-AES or ICP-MS if required]), Code 6 HR-ICP-MS (Water analysis by High Resolution ICP-MS), Code 6 Au HR-ICP-MS (Au by High Resolution ICP-MS), and Code 6 Boron (Boron add-on by ICP-MS).

Data availability

All data generated or analysed during this study are included in this published article and supplementary information files.

Received: 16 November 2023; Accepted: 4 March 2024

Published online: 08 March 2024

References

- United States Geological Survey (USGS). *Mineral Commodity Summaries 2023*, USGS, USA 214 (2023).
- Hedenquist, J. W., Izawa, E., Arribas, A. & White, N. C. Epithermal gold deposits: Styles, characteristics and exploration. *Soc. Resour. Geol. Spec. Pub.* **1**, 1–17 (1996).
- Groves, D. I., Goldfarb, R. J., Gebre-Mariam, M., Hagemann, S. G. & Robert, F. Orogenic gold deposits: A proposed classification in the context of their crustal distribution and relationship to other gold deposit types. *Ore Geol. Rev.* **13**, 7–27 (1998).
- Phillips, G. N. & Powell, R. Formation of gold deposits: Review and evaluation of the continuum model. *Earth-Sci. Rev.* **94**, 1–21 (2009).
- Mercier-Langevin, P., Hannington, M. D., Dubé, B. & Bécu, V. The gold content of volcanogenic massive sulfide deposits. *Mineral. Deposita* **46**, 509–539 (2011).
- Sillitoe, R. H. Gold deposit types: An overview. *Soc. Econ. Geol. Spec. Pub.* **23**, 1–28 (2020).
- Volesky, B. & Holant, Z. R. Biosorption of heavy metals. *Biotechnol. Prog.* **11**, 235–250 (1995).
- Kratochvil, D. & Volesky, B. Advances in the biosorption of heavy metals. *Trends Biotechnol.* **16**, 291–300 (1998).
- Das, N., Vimala, R. & Karthika, P. Biosorption of heavy metals—an overview. *Indian J. Biotechnol.* **7**, 159–169 (2008).
- Abbas, S. H., Ismail, I. M., Mostafa, T. M. & Sulaymon, A. H. Biosorption of heavy metals: A review. *J. Chem. Sci. Technol.* **3**, 74–102 (2014).
- Ordóñez, J. I., Cortés, S., Maluenda, P. & Soto, I. Biosorption of heavy metals with algae: Critical review of its application in real effluents. *Sustainability* **15**, 5521 (2023).
- Konishi, Y. *et al.* Microbial deposition of gold nanoparticles by the metal-reducing bacterium *Shewanella algae*. *Electrochim. Acta* **53**, 186–192 (2007).
- Shankar, P. D. *et al.* A review on the biosynthesis of metallic nanoparticles (gold and silver) using bio-components of microalgae: Formation mechanism and applications. *Enzyme Microb. Technol.* **95**, 28–44 (2016).
- Menon, S., Rajeshkumar, S. & Kumar, V. A review on biogenic synthesis of gold nanoparticles, characterization, and its applications. *Resour.-Eff. Technol.* **3**, 516–527 (2017).
- Khan, A. U., Khan, M., Malik, N., Cho, M. H. & Khan, M. M. Recent progress of algae and blue-green algae-assisted synthesis of gold nanoparticles for various applications. *Bioprocess. Biosyst. Eng.* **42**, 1–15 (2019).
- Fujita, T., Kuzuno, E. & Mamiya, M. Adsorption of metal ions by river algae. *Shigen-to-Sozai* **108**, 123–128 (1992).
- Fukushima, Y. & Murao, S. Gold recovery from tailings by using blue-green algae. In *Proc. 32th Symp. Geo-Environ. Geo-Tech* 127–130 (2022).
- Fukushima, Y., Sakai, T., Takahashi, K., Kadowaki, H. & Fujita, T. Biosorption technology for valuable metals recovery by using biosorbents made from blue-green algae. *Shigen-Chishitsu* **74**, xxx–xxx (in press).
- Mariko, T. *Economic Geology: Geoscience for Metal Resources*, Kokon-Shoin, Japan 580 (2008).
- Muto, N. & Matsubaya, O. Origin and geochemical variation of geothermal water in the Tamagawa Hot Spring area, Akita, Japan. *Chikyu-Kagaku (Geochem.)* **36**, 81–88 (2002).
- Yoshiike, Y. Variation in the chemical composition of Obuki Spring, Tamagawa Hot Springs (1951–2000). *Geochem. J.* **37**, 649–662 (2003).
- Sanada, T., Takamatsu, N. & Yoshiike, Y. Geochemical interpretation of long-term variations in rare earth element concentrations in acidic hot spring waters from the Tamagawa geothermal area, Japan. *Geothermics* **35**, 141–155 (2006).
- Sato, H., Ishiyama, D., Mizuta, T., Matsubaya, O. & Murakami, F. Geochemical characteristics of thermal waters and precipitates in Tamagawa Hot Spring area, Akita, Japan. *Shigen-Chishitsu* **60**, 15–24 (2010).
- Ogawa, Y. *et al.* Fractionation and deposition of indium and arsenic from the Kussatsu and Tamagawa acidic hot springs, Japan: Possible man-made analogues for rare metal concentrations onto Lake Beds? *Econ. Geol.* **108**, 1641–1656 (2013).
- Ansai, T. & Inoue, H. Sulphur deposits on Western Hachimantai Plateau. *Bull. Geol. Surv. Jpn.* **5**, 23–34 (1954).
- Sasaki, N., Yamashita, A. & Watanuki, K. The chemical composition of plumbian barite (hokutolite) precipitated from 1981 to 1990 at Tamagawa Hot Springs, Akita Prefecture, Japan. *Mineral. J.* **16**, 49–59 (1992).
- Shenberger, D. M. & Barnes, H. L. Solubility of gold in aqueous sulfide solutions from 150 to 350°C. *Geochim. Cosmochim. Acta* **53**, 269–278 (1989).
- Fuchs, S., Hannington, M. D. & Petersen, S. Divining gold in seafloor polymetallic massive sulfide systems. *Mineral. Deposita* **54**, 789–820 (2019).
- Alviani, V. N. *et al.* Local initiative hydrogen production by utilization of aluminum waste materials and natural acidic hot-spring water. *Appl. Energy* **293**, 116909 (2021).
- Okada, S., Chen, C., Watanabe, H. K., Isobe, N. & Takai, K. Unusual bromine enrichment in the gastric mill and setae of the hadal amphipod *Hirondellea gigas*. *PLoS ONE* **17**, e0272032 (2022).
- Takaya, Y. *et al.* The tremendous potential of deep-sea mud as a source of rare-earth elements. *Sci. Rep.* **8**, 5763 (2018).
- Nozaki, T. *et al.* Formation of highly Zn-enriched sulfide scale at a deep-sea artificial hydrothermal vent, Iheya-North Knoll, Okinawa Trough. *Mineral. Deposita* **56**, 975–990 (2021).
- Miyazaki, J. *et al.* Deepest and hottest hydrothermal activity in the Okinawa Trough: The Yokosuka site at Yaeyama Knoll. *R. Soc. Open Sci.* **4**, 171570 (2017).
- Nozaki, T. *et al.* Rapid growth of mineral deposits at artificial seafloor hydrothermal vents. *Sci. Rep.* **6**, 22163 (2016).
- Takahashi, Y. *et al.* Investigation report of opal occurring at Shinyu, Tateyama Hot Spring. *Bull. Tateyama Caldera Sabo Mus.* **8**, 1–4 (2007).
- Jette, E. R. & Foote, F. Precision determination of lattice constants. *J. Chem. Phys.* **3**, 605–616 (1935).
- Thanh, N. T. K., Maclean, N. & Mahiddine, S. Mechanisms of nucleation and growth of nanoparticles in solution. *Chem. Rev.* **114**, 7610–7630 (2014).

38. Du, K., Hochmeister, K. V. & Phillipp, F. Quantitative comparison of image contrast and pattern between experimental and simulated high-resolution transmission electron micrographs. *Ultramicroscopy* **107**, 281–292 (2007).

Acknowledgements

We thank Y. Otsuki of JAMSTEC for her assistance with the ICP-MS analysis. Discussion with T. Nagase of Tohoku University was fruitful. We are grateful to N. Tsuchiya, M. Oba, and N. Hirano of Tohoku University, K. Nakazawa of DOWA Techno Engineering Co., LTD, S. Narita and K. Taiyoshi of the Tamagawa Dam Management Office, Tohoku Regional Development Bureau, Ministry of Land, Infrastructure, Transport and Tourism for their approval and special support for the in situ Au gold experiment. This work was supported by JSPS KAKENHI Grant Numbers 23H03812 and 23H01914 to T.N. and by a grant from the Canon Research Foundation to T.N.

Author contributions

T.N. and Y.F. conceived the idea of this study. Y.F. incubated and produced the blue-green algae sheet. T.N., Y.F., S.O., and M.W. conducted the in situ Au adsorption experiments. S.O. performed the FE-SEM observations. T.N. and Y.T. performed the ICP-MS analysis of blue-green algae sheets and hot spring water. A.M. carried out the ICP-AES analysis of natural hot spring water. T.N. mainly wrote the manuscript with inputs from all authors.

Competing interests

The authors declare no competing interests.

Additional information

Supplementary Information The online version contains supplementary material available at <https://doi.org/10.1038/s41598-024-56263-3>.

Correspondence and requests for materials should be addressed to T.N.

Reprints and permissions information is available at www.nature.com/reprints.

Publisher's note Springer Nature remains neutral with regard to jurisdictional claims in published maps and institutional affiliations.



Open Access This article is licensed under a Creative Commons Attribution 4.0 International License, which permits use, sharing, adaptation, distribution and reproduction in any medium or format, as long as you give appropriate credit to the original author(s) and the source, provide a link to the Creative Commons licence, and indicate if changes were made. The images or other third party material in this article are included in the article's Creative Commons licence, unless indicated otherwise in a credit line to the material. If material is not included in the article's Creative Commons licence and your intended use is not permitted by statutory regulation or exceeds the permitted use, you will need to obtain permission directly from the copyright holder. To view a copy of this licence, visit <http://creativecommons.org/licenses/by/4.0/>.

© The Author(s) 2024